2025 SPE Western Regional Meeting

SPE-224132-MS

Optimizing Power Fluid in Jet Pump Oil Wells

Kaelin W. Ellis[1, 2] and **Obadare O. Awoleke**[2]

[1]Hilcorp Alaska, Anchorage, AK, USA

[2]University of Alaska, Fairbanks, AK, USA

Abstract

A method for optimizing power fluid to a network of jet pump wells is established. Jet pump performance is modeled by numerically solving a system of equations for specific throat and nozzle geometries. An upper boundary is established of the most efficient geometries for each well which creates a continuous function relating power fluid to oil production. Jet pump oil wells are segregated into networks which share a common power fluid surface pump. These boundaries are added together to create a non-linear objective function. To solve power fluid distribution in a network, a reduced Newton method is applied that incorporates active constraints. System constraints are that the total network power fluid is at or below surface pump capacity and that each power fluid rate is non-negative. Upon successful convergence, the power fluid estimate per well is passed to a discrete algorithm to choose between either a high or low power fluid jet pump.

A computer program is developed capable of implementing the optimization method. This program is successfully tested on an eight well network, determining whether an additional well can be supported with existing equipment. The continuous optimization is fast, converging in four iterations to an answer. Results from a discrete algorithm are displayed with individual oil well jet pump geometries. Any engineer can run this program, providing the benefit of a unified approach to decision making. This is a significant improvement, since no previous methods have been found in literature on how to distribute power fluid across a jet pump network.

Introduction

Jet pumps are a very viable form of artificial lift in cold shallow reservoirs. A jet pump poses quite a few advantages over alternative methods such as gas lift or electric submersible pumps. These advantages include warming production fluid with annular heat transfer, gas handling capability, and ease of replacement. Despite these advantages, no unified method has been proposed for how to properly distribute power fluid among different wells. This becomes critical as more wells are added to existing infrastructure and the available surface pump capacity needs to be allocated.

A reliable optimization method requires an accurate system model. Despite its simple appearance, an oil well jet pump needs advanced fluid mechanics for modeling. First principle analytical models of two-phase flow in jet pumps were pioneered by Cunningham (1995). These models quantified the impact of gas handling with sonic choking at the throat entrance. Though equations derived in Cunningham's work are impeccable, assumptions used are ideal gas, incompressible and non-gas soluble liquids. These assumptions are not valid for an oil reservoir fluids mixture and more robust modeling is required.

Numerical methods are well poised to handle complex equations that cannot take advantage of simplifying assumptions. For a jet pump in an oil well, the first documented application is by Merrill et al. (2020). In this work, methods are provided for how to estimate a reservoir fluid's change in energy due to expansion and interpreting choked flow conditions. In upcoming sections, novel applications of numerical methods are introduced with two new algorithms. The first algorithm is for calculating the minimum theoretical suction pressure of a jet pump. The second algorithm is for converging to a jet pump solution with the required inflow and outflow conditions.

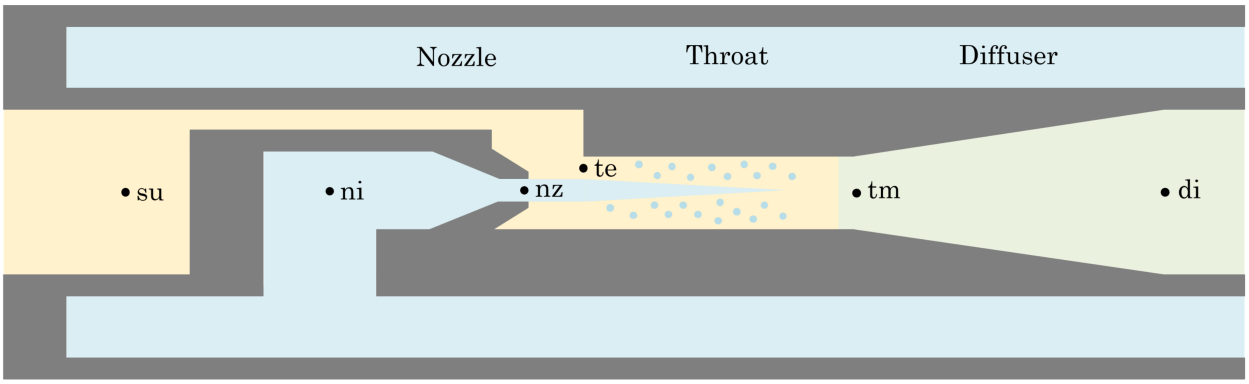

Figure 1: Jet Pump Overview

The goal of power fluid optimization is to maximize total oil production from the available power fluid supply. Using standard jet pump oil well nozzle and throat combinations an upper boundary is established that relates oil production to power fluid for each well. All the boundaries together create a non-linear function with individual power fluid usage per well as the input. Upon completion, optimized power fluid rates are passed to a discrete algorithm that selects the specific jet pump geometries. An example concludes the paper with properly selecting power fluid rate and jet pump geometries in an eight well power fluid network.

Jet Pump Theory

A jet pump is made up of three mechanical components which are a nozzle, throat and diffuser. Six reference locations are assigned inside the jet pump for differences in pressure and fluid properties. Reference locations are the suction (su), nozzle inlet (ni), nozzle tip (nz), throat entrance (te), throat mixture (tm) and diffuser outlet (di). Figure 1 provides a diagram for jet pump geometry.

Fluid Equation

The one-dimensional fluid energy equation provides the foundation for compressible flow in conduits (Holland and Bragg 1995). The energy equation states that the differences in potential energy, pressure energy, kinetic energy, friction and work have to be equal. For a jet pump, potential energy and work terms can be omitted. The fluid energy equation simplifies to the jet pump energy equation (1).

$$\frac{dP}{\rho} + VdV + dF = 0 \tag{1}$$

Fluid flow across a jet pump nozzle tip, throat entrance and diffuser can all be modeled using variations of the jet pump energy equation. Equations associated with the different components are detailed in the next sections. Detailed derivations for these equations are provided in Appendix A, B, C and D. Cunningham (1974) also provides a useful overview of equations and their derivations for liquid jet gas pumps.

Throat Entrance

Reservoir fluids enter a jet pump by way of the throat entrance. As seen in figure 1 the throat entrance is constricted by the power fluid jet. An increase in velocity occurs, transforming pressure energy into kinetic energy. Reservoir fluid is a non-ideal three phase mixture with gas continually liberating from the liquid. As such, minimal assumptions can be applied to the fluid energy equation to simplify it. Only an assumption of negligible suction velocity is used. Equation (1), jet pump energy, is rewritten specifically for a throat entrance as equation (2).

$$E_{te} = \int_{su}^{te} \frac{dP}{\rho} + \frac{V_{te}^2}{2} * (1 + K_{en}) = 0 \tag{2}$$

E_{te} stands for energy of the throat entrance, calculating the difference in energy between the fluid at the suction and at the throat entrance. To have physical meaning, E_{te} needs to equal zero. In the numerical solution section of this paper, the integral is converted to a summation with the trapezoid rule. This allows for pressure at the throat entrance to be calculated.

Nozzle

Water is used as power fluid for flow across the jet pump nozzle. Water is incompressible and velocity at the nozzle inlet is negligible. These simplifications allow the jet pump energy equation to be analytically integrated for all the terms. Pressure at the throat entrance, P_{te}, is equal to the pressure at the nozzle tip, P_{nz}. These steps yield equation (3).

$$P_{te} = P_{ni} - \frac{\rho_{nz} V_{nz}^2}{2} * (1 + K_{nz}) \tag{3}$$

In practice, P_{te} is solved by analyzing the throat entrance. Once a numerical solution of P_{te} is made, the nozzle equation is used to calculate the velocity and flow rate of the power fluid.

Throat

A jet of power fluid congregates with reservoir fluids inside the throat. Momentum is transferred from power fluid into reservoir fluids, causing an increase in pressure. Mass flow, velocity and pressure at the inlet and outlet of the throat are balanced with each other. Final simplification yields equation (4).

$$P_{te} - P_{tm} = \frac{\rho_{tm} V_{tm}^2 K_{th}}{2} + \frac{\dot{m}_{tm} V_{tm}}{A_{th}} - \frac{\dot{m}_{nz} V_{nz}}{A_{th}} - \frac{\dot{m}_{te} V_{te}}{A_{th}} \tag{4}$$

Density and velocity at the throat outlet are dependent on the outlet pressure. Due to the implicit nature of the equation an iterative loop is required. The numerical methods section provides detail for the secant method application to solve for P_{tm}.

Diffuser

Kinetic energy is converted back into pressure energy at the diffuser. This results in a condition that is similar to the throat entrance. One difference though is velocity at the throat mixture is not negligible and must be included in the calculation. Solving the fluid equation for the diffuser yields equation (5).

$$E_{di} = \int_{tm}^{di} \frac{dP}{\rho} + \frac{V_{di}^2}{2} - \frac{V_{tm}^2}{2} * (1 + K_{di}) = 0 \tag{5}$$

Fluid inside the diffuser is a mixture of power and reservoir fluid, preventing analytical integration. In appendix D, the integral is converted to a summation with the trapezoid rule. This allows for pressure at the diffuser to be calculated.

Applied Oil Well Model

In the previous section equations are introduced for a liquid jet multiphase pump. Complex behavior regarding density of a reservoir fluid make an analytical solution difficult. In the following section numerical methods are introduced to provide solutions for P_{te}, P_{tm} and P_{di}. Solutions are linked backed to an oil well's inflow performance and well bore geometry to provide a solution for the entire well.

Figure 2 is a diagram of a jet pump inside an oil well. As shown, a jet pump has three boundary conditions to meet, which are P_{su}, P_{ni} and P_{di}. Pressure drop in the well annulus is assumed to be negligible, so nozzle inlet pressure is only dependent on the surface delivery and static pressure. Discharge pressure needs to overcome the static and frictional pressure loss in the tubing, which will be covered in a later section. Suction pressure is defined using reservoir inflow performance.

An inflow performance relationship (IPR) provides an estimate of how much fluid will be produced for a given suction pressure, also known as the wells flowing bottom hole pressure, P_{wf}. Any method can be used to define the IPR as long as

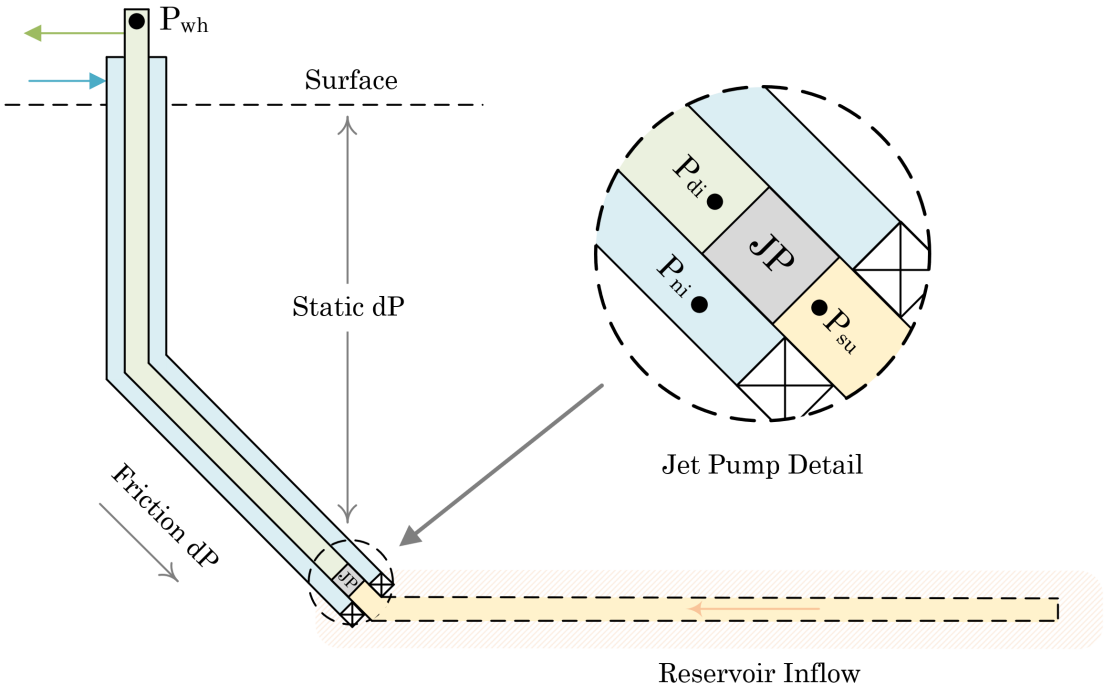

Figure 2: Jet Pump Well Assembly

reservoir fluid flow is calculated at various bottom hole pressures. In this analysis Vogel (1968) is applied for an estimate of the well's inflow performance.

Throat Entrance

Defining an initial suction pressure with an IPR provides an estimate of reservoir flow rate. For multiphase mixtures, the sonic velocity is much less than its individual components (Himr et al. 2009). This causes jet pumps to be prone to hitting a sonic limit at the throat entrance (Verma et al. 2014). Reservoir inflow and sonic velocity create an upper and lower boundary on the throat entry pressure. These boundaries govern the total solution for the jet pump and do not depend on any other components. The significant influence of the throat entrance make it an ideal starting point for solving the jet pump system of equations.

As previously stated, an analytical solution for the change in density of a reservoir fluid related to pressure is cumbersome. The trapezoid rule is applied to numerically find a solution of an integral (Gilat and Subramaniam 2013). In equation (6), trapezoid rule summation notation replaces the integral of equation (2).

$$E_{te} = \underbrace{\frac{\Delta P}{2} \sum_{k=su}^{te} \left(\frac{1}{\rho_k} + \frac{1}{\rho_{k+1}}\right)}_{\text{Expansion Energy}} + \underbrace{\frac{V_{te}^2}{2} * (1 + K_{en})}_{\text{Kinetic Energy}} = 0 \tag{6}$$

Equation 6 is broken into two distinct portions, expansion energy and kinetic energy. Expansion describes the fluid's energy from differences in density due to pressure changes. Kinetic describes the fluid's energy from velocity and losses to friction. A solution is reached when a throat entry pressure is calculated that balances expansion energy leaving the fluid with kinetic energy entering the fluid.

Figure 3 is a graphical representation applying equation (6) to find a solution across the throat entrance. For a given well, a suction pressure is selected, which drives reservoir fluid flow rate and mixture properties. Suction pressure is viewed as the highest pressure on figure 3. At each iteration suction pressure is reduced by a delta pressure, ΔP, until a condition is met causing it to stop. A detailed explanation of the method and stopping conditions are shown in an algorithm below.

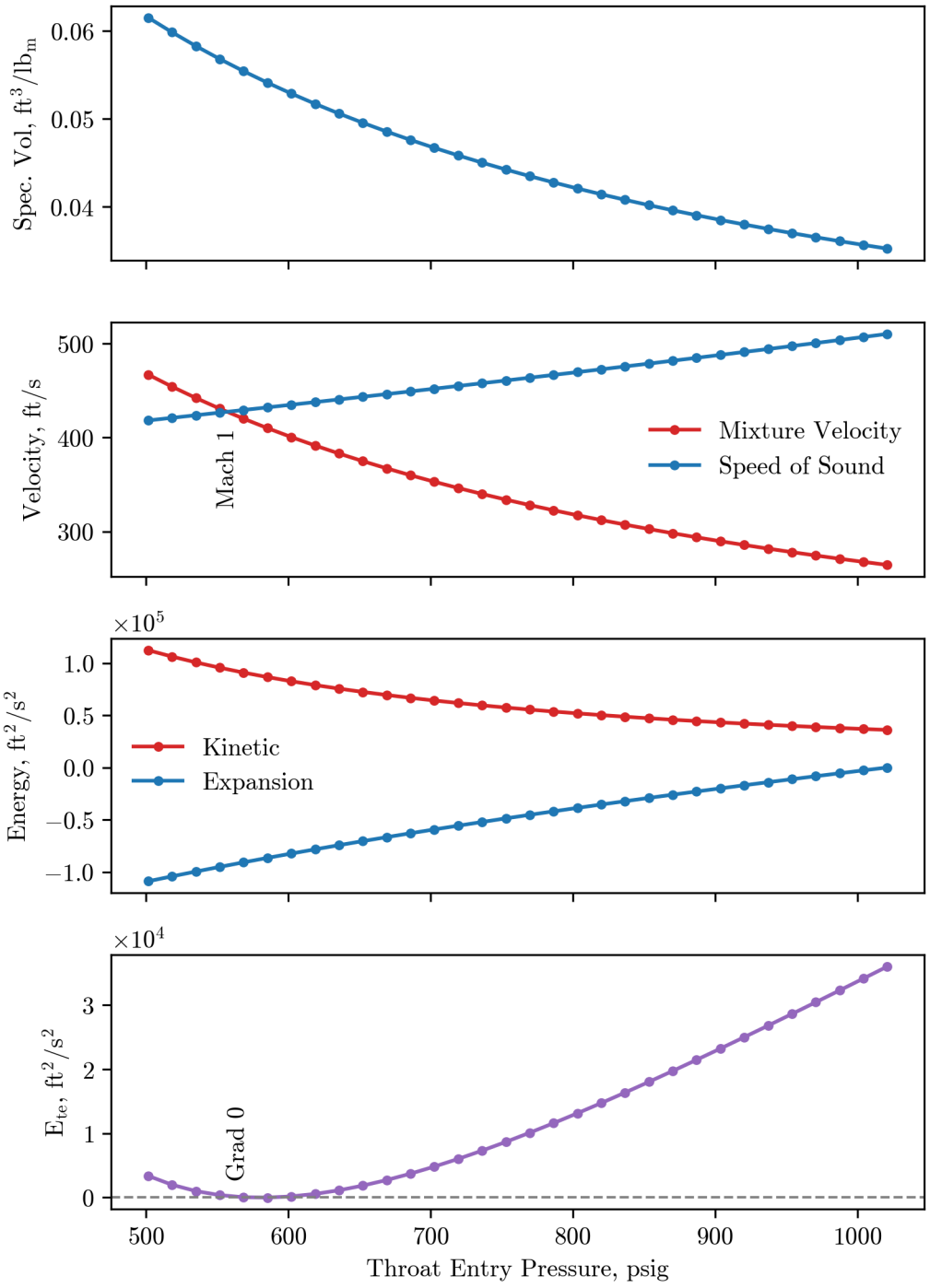

Figure 3: Properties for Calculating Throat Entry Pressure

Algorithm 1: Throat Entry Pressure

1. Select guess suction pressure, P_{su} and pressure delta, ΔP
2. $P_0 = P_{su}$
3. For $k = 0, 1, ...$
   (a) $P_{k+1} = P_k - \Delta P$
   (b) $V_{te} = V_{k+1}$
   (c) Calculate E_{te} and Ma
   (d) Four outcomes are possible
      i. $E_{te} > 0$ and Ma < 1. Repeat Loop, $k = k + 1$
      ii. $E_{te} > 0$ and Ma ≥ 1. Stop, restart with higher suction pressure
      iii. $E_{te} \leq 0$ and Ma < 1. Stop, a non-choked solution is found. $P_{te} = P_k$
      iv. $E_{te} \leq 0$ and Ma ≥ 1. Stop, a choked solution is found. $P_{te} = P_k$

In practice, pressure reductions rarely land where E_{te} is exactly equal to zero. Interpolation is used to calculate the pressure where E_{te} is zero. A smaller ΔP can be used to reduce this error but requires more computational power. In figure 3 a choked solution was found, where both $E_{te} = 0$ and Ma $= 1$. At the solution $P_{te} \approx 575$ psig. As seen in the graph of E_{te} at Mach one the gradient is zero. This is due to the transition from subsonic to sonic flow, represented by equation (7). A derivation is provided in appendix E.

$$\frac{dE_{te}}{dP} = \frac{1}{\rho}(1 - \text{Ma}^2) \tag{7}$$

The choked solution where $E_{te} = 0$ and Ma $= 1$ is significant because it provides the theoretical lowest suction pressure for a given reservoir inflow and jet pump geometry. Once a jet pump is choked, no reduction in discharge pressure will result in more flow through the pump. When solving the jet pump solution, it is advantageous to start with finding the suction pressure that provides choked flow at the throat entry. The secant method is an iterative method that finds where a function is equal to zero (Gilat and Subramaniam 2013). It is well suited for finding where E_{te} is zero at Mach one and is shown in the algorithm below.

Algorithm 2: Lowest Theoretical Suction Pressure

1. Select two guess suction pressures P_{su}^0 and P_{su}^1.
2. Calculate E_{te}^0 at Ma= 1 and E_{te}^1 at Ma= 1.
3. For $k = 1, 2, ...$
   (a) $P_{su}^{k+1} = P_{su}^k - E_{te}^k \dfrac{P_{su}^k - P_{su}^{k-1}}{E_{te}^k - E_{te}^{k-1}}$
   (b) Calculate E_{te}^{k+1} at Ma= 1
   (c) Stop when $E_{te}^{k+1} = 0$ at Ma= 1
   (d) $k = k + 1$

Figure 4 is an example of E_{te} at five different suction pressures. The wells water cut and gas oil ratio are assumed to be constant for different suction pressures. Formation water and gas volumes are used for calculating V_{te} but are omitted in the legend to reduce clutter on the graph. Only produced oil volume at each suction pressure is displayed. Various suction pressures are equally spaced for clarity. As seen, the orange line is associated with a solution at a choked entrance, which would be found in the previously described algorithm. The green, red and purple lines cross the 0 axis prior to choking, which results in an un-choked solution. The blue line does not cross the 0 axis prior to choking, meaning the selected suction pressure was too low, resulting in too much flow.

Nozzle, Throat and Diffuser

Once a solution for P_{te} is obtained, solutions for equations across the nozzle, throat and diffuser are completed. Extensive discussions for these components are not required, as the behavior is not as complex as the throat entry. Nozzle inlet pressure is obtained from statics and P_{nz} is assumed to be equal to P_{te}. This leaves the associated nozzle velocity to be solved for. The throat is inherently implicit since the properties at the outlet of the throat are dependent on P_{tm}. The throat equation

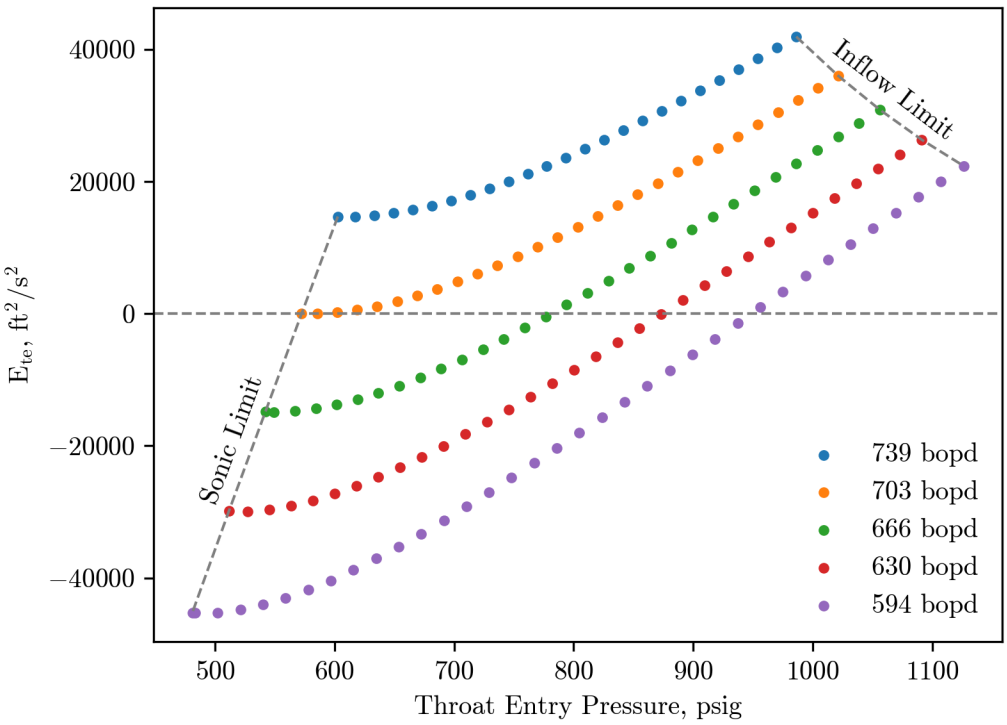

Figure 4: Energy of the Throat Entrance at Multiple Suction Pressures

is rewritten in the form $f(P_{tm}) = 0$ by moving parameters to the left. Using the secant method, P_{tm} is iterated until a solution is found.

The diffuser is the final piece to be calculated. It is solved with the same numerical method as the throat entrance. Instead of decreasing pressure until $E_{di} = 0$, pressure is increased in increments of ΔP. A diffuser also has the benefit that sonic choking is not a concern. This is due to the the large influx of water into reservoir fluid from the nozzle jet. Water drastically raises the mixture sonic velocity. A solution for diffuser pressure, P_{di}, is obtained where $E_{di} = 0$.

Outflow Considerations

At this point, a solution has been obtained that meets geometrical constraints of the jet pump and inflow constraints of the reservoir. Outflow conditions of the well ensure that the prescribed jet pump can lift reservoir fluids to surface. Two separate terms will be defined, the first being available discharge pressure, defined as P_{di}^{A}. Available discharge pressure is what was calculated in the previous sections and it's how much discharge pressure can be provided for a given jet pump and inflow conditions.

The second term is required discharge pressure, defined as P_{di}^{R}. Required discharge pressure describes pressure needed to lift the fluid from the jet pump to the well head. It includes wellhead pressure, static and frictional pressure gradient in the well. The required discharge pressure is written in equation 8.

$$P_{di}^{R} = P_{wh} + P_{fric} + P_{static} \tag{8}$$

Variables are well head pressure, frictional pressure loss in tubing and static pressure loss. Though the majority of fluid in tubing is water, free gas still exists and multiphase correlations are used. Beggs and Brill (Payne et al. 1979) is used to calculate static and frictional pressure drop. A term called discharge residual is created to compare the available and required discharge pressure.

$$R_{di} = P_{di}^{A} - P_{di}^{R} \tag{9}$$

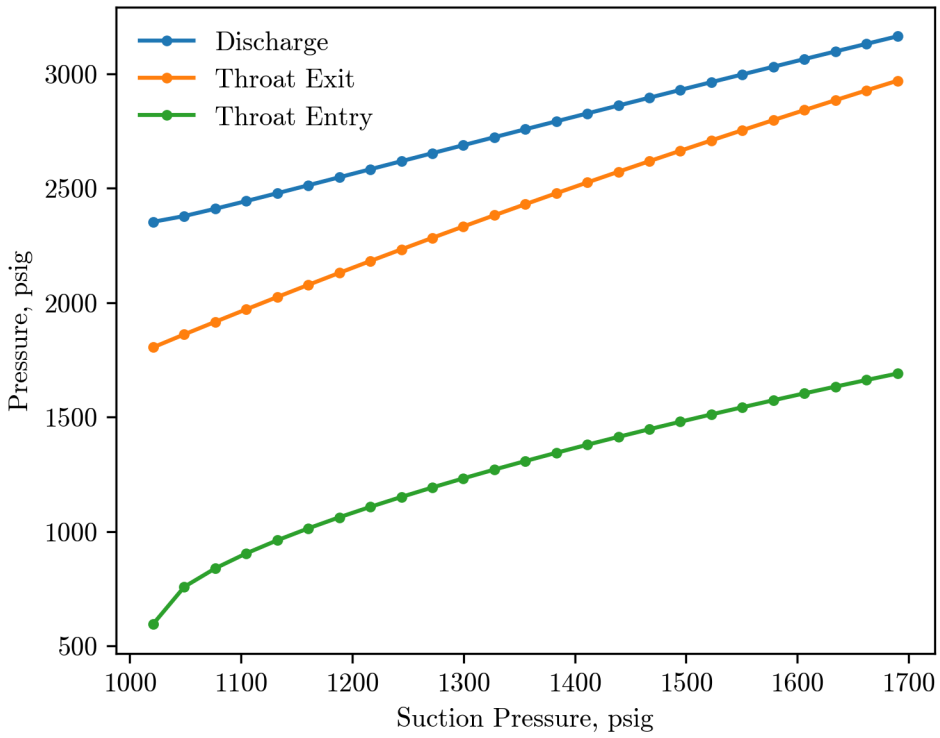

Figure 5: Pressure Relation from Varying Suction Pressure

For a given jet pump operating at a specific well head and power fluid pressure, discharge residual is only dependent on a pump's suction pressure. Similar to previous sections, a numerical scheme is deployed to find a suction pressure where $R_{di} = 0$. Suction pressure where $R_{di} = 0$ occurs between two extremes, the minimum and maximum. Minimum suction pressure is where the throat entrance is operating in choked flow. Maximum suction pressure uses a ten psi draw down across the reservoir. An algorithm for finding where the residual is zero is detailed below.

Algorithm 3: Solution for Jet Pump Oil Well Assembly

1. Calculate P_{su}^0, Suction pressure of a choked jet pump
2. Calculate R_{di}^0
   (a) If $R_{di}^0 \geq 0$, Stop, a choked solution is found.
3. Calculate $P_{su}^1 = P_{re} - 10$, Reservoir pressure with 10 psig of drawdown.
4. Calculate R_{di}^1
   (a) If $R_{di}^1 < 0$, Stop, well cannot flow to surface.
5. For $k = 1, 2, ...$
   (a) $P_{su}^{k+1} = P_{su}^k - R_{di}^k \dfrac{P_{su}^k - P_{su}^{k-1}}{R_{di}^k - R_{di}^{k-1}}$
   (b) Stop when $R_{di}^{k+1} = 0$
   (c) $k = k + 1$

Figure 5 shows the relationship between suction pressure of the jet pump and the discharge. Despite throat entry pressure not being linear to suction, the discharge is quite linear. The secant method takes advantage of this relationship to quickly iterate to a solution that drives discharge residual to zero. Now that a jet pump model has been completed, it can be deployed to quickly understand performance of different jet pumps in an oil well.

Jet Pump Specifics

Background on jet pump nomenclature is provided to assist in continuing the discussion. Jet pumps are identified by a nozzle number and a throat ratio. In this analysis, the National standard pump geometry will be used, which can be referenced in Petrie et al. (1983a). Nozzle number is an integer with a value of 1 to 20, each corresponding to a specific diameter. Throat ratio is a letter of the form X, A, B, C, D or E which is throat diameter divided by nozzle diameter. An example of identification is 11X, 13C, or 9D. Table 1 shows numeric ratios at each letter.

Ratio	Nozzle	Throat	Area Ratio	Dia. Ratio
X	N	N - 1	2.07	1.44
A	N	N	2.63	1.62
B	N	N + 1	3.34	1.83
C	N	N + 2	4.26	2.06
D	N	N + 3	5.43	2.33
E	N	N + 4	6.90	2.63

Table 1: Jet Pump Throat to Nozzle Ratios

Specifying jet pumps in this manner allows quick generalities to be made about their behavior. An X pump provides the largest head, but the smallest suction flow for a given nozzle. Likewise, an E provides the smallest head, but the largest suction flow for a given nozzle. Selection of a specific nozzle number from National standard tables allows a throat to be referenced directly for a specific ratio. shown in table 1. For example, an 11X corresponds to an 11 nozzle with a 10 throat. A 13C would correspond to a 13 nozzle with a 15 throat.

In previous equations, frictional coefficients for jet pumps are displayed with no discussion on reasonable values. Frictional values used are based on two separate studies. First is by Sanger (1968) from studying liquid jet liquid pumps. Values proposed by Sanger are in table 2 for the throat entrance and the nozzle. Second is by Cunningham (1995) from studying liquid jet gas pumps. Values proposed by Cunningham are in table 2 for the throat and diffuser.

Description	Symbol	Value
Throat Entrance	K_{te}	0.03
Nozzle	K_{nz}	0.01
Throat	K_{th}	0.3
Diffuser	K_{di}	0.3

Table 2: Model Friction Coefficients

Live data of suction and discharge pressure gauges in a select group of wells was compared to model results using friction values in table 2. An adequate match was obtained comparing the model with field data to feel confident carrying the frictional values forward.

Batch Jet Pump Runs

Assessing a single jet pump provides little context to help optimize power fluid for a well. Power fluid pressure for each well can be reduced with an individual surface choke, which would reduce power fluid rate. The problem with choking pressure is that it wastes valuable energy required to increase pressure. A better approach is to replace the subsurface jet pump to meet required operating conditions. Controlling power fluid flow with the jet pump nozzle tip ensures that the max pressure is delivered to each well.

A batch run method is used on each oil well to run an array of multiple jet pumps. If desired, every nozzle and throat combination from the National pump standard could be run, but this is excessive. On Alaska's North Slope the largest and smallest jet pump sizes are 14C and 8B respectively. For a batch run nozzle sizes selected are seven to sixteen and throat ratios are X, A, B, C, D and E. This ensures all potential combinations are covered and provides edge cases.

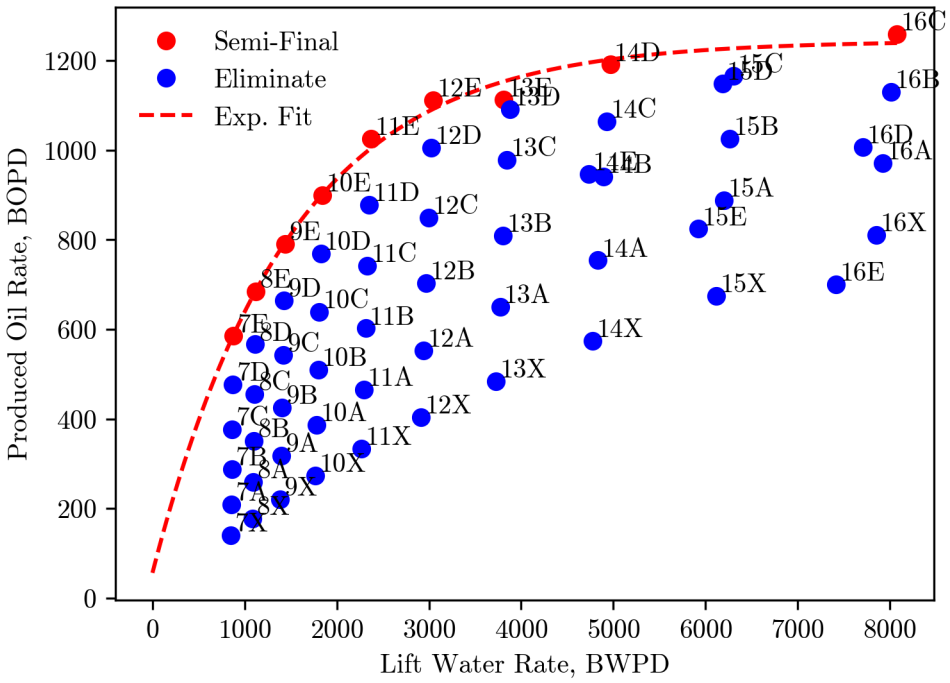

Figure 6: Batch Run Results

Result of a batch run for a well on the North Slope is shown in figure 6. Jet pumps are segregated into semi-finalist, red dots, and eliminated, blue dots. Jet pumps are deemed a semi-finalist if no other jet pump can make more oil for less water produced. This ensures any additional power fluid, also known as lift water, will yield more oil for a given jet pump. A curve is fitted along semi-finalists which provides an analytical equation to describe the increase in oil rate for a given power fluid volume. The curve fit is shown as equation (10).

$$q_o = c_1 - c_2 \exp\left(-q_p c_3\right) \tag{10}$$

Coefficients c_1, c_2 and c_3 are found with a non-linear curve fit. The benefit of the curve fit is that a derivative can easily be taken to describe marginal increase in oil rate for a marginal increase in power fluid. This concept is foundational to the optimization scheme. No jet pumps are considered inside the optimization scheme other than the semi-finalists.

Network Optimization

A jet pump network is defined as a collection of oil wells that share a surface power fluid pump. The power fluid pump is responsible for taking spent power fluid from a well and increasing pressure to be reused. Depending on the installation, these pumps normally operate at max capacity. Figure 7 shows a network of four jet pump wells that are reliant on the same surface pump. The optimization objective function and constraints take the form:

$$\begin{aligned} \text{maximize } & f(q_p) = \sum_{i=1}^{n} q_{o\,i} \\ \text{subject to } & \sum_{i=1}^{n} q_{p\,i} \leq Q_{\text{p}}^{\text{pump}} \\ & q_{p\,i} \geq 0 \end{aligned}$$

Index i represents a specific unique oil well that is on the network, with n being the total number of wells. Vector q_p represents the individual power fluid to each well $q_p = (q_{p\,1}, q_{p\,2}, ..., q_{p\,n})^T$. Power fluid supplied to each well must sum up to less than or equal the surface pump capacity and each power fluid must be non-negative.

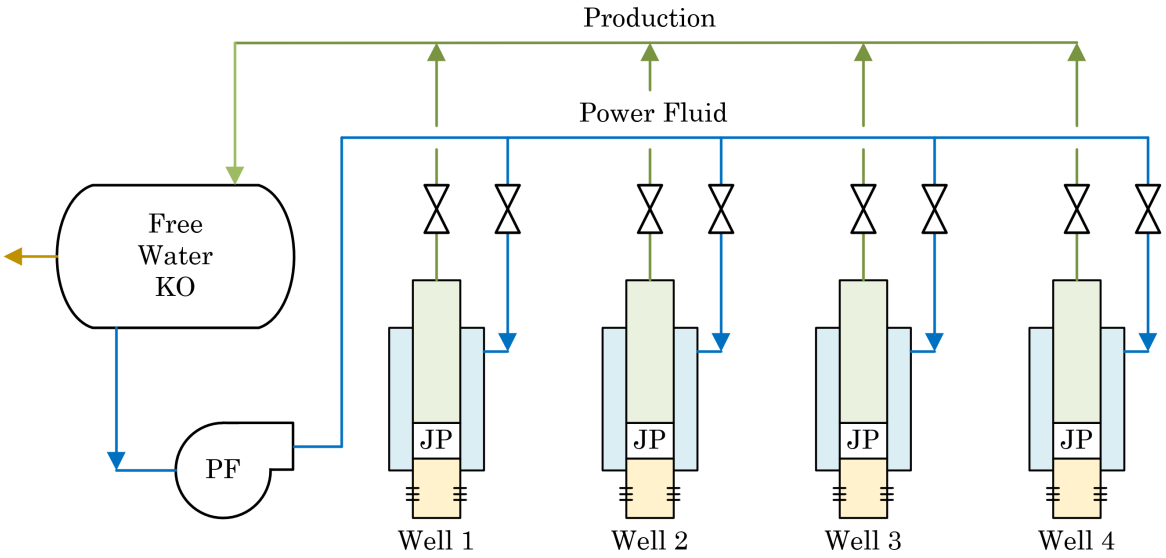

Figure 7: Network Diagram of Four Wells

Reduced Newton's Method with Active Set Constraints

A reduced Newton method is used for finding direction, while an active set is used to handle constraints. The active set method is solving a problem of the form:

$$\begin{aligned} &\text{minimize } f(x) \\ &\text{subject to } \hat{A}x = \hat{b} \end{aligned}$$

The function $f(x)$ is any non-linear function while $\hat{A}$ and $\hat{b}$ are the active inequality and equality constraints. The null space of $\hat{A}$ is defined as $\hat{Z}$ and is used to reduce the gradient and Hessian of the objective function. The reduction ensures travel direction, p, does not violate any currently active constraints. The reduced gradient, $\nabla\phi(v)$ and Hessian, $\nabla^2\phi(v)$ are shown using under braces. Equation (11) is referred to as the *reduced Newton direction*.

$$p = \hat{Z}v = -\hat{Z}(\underbrace{\hat{Z}^T\nabla^2 f(x_k)\hat{Z}}_{\nabla^2\phi(v)})^{-1}\underbrace{\hat{Z}^T\nabla f(x_k)}_{\nabla\phi(v)} \tag{11}$$

A backtracking line search from Armijo (1966) is used to estimate a step size that guarantees descent of the objective function. The ratio test ensures that a step size does not exceed any inactive constraints. Active constraints are continually assessed with Lagrange multiples to ensure they aren't preventing further objective function minimization while remaining feasible. Using results of the ratio test and Lagrange multiples, the active set $\hat{A}$, $\hat{b}$ and the null space $\hat{Z}$ are updated. The program terminates once an optimal condition is achieved, shown in equation (12).

$$\| \hat{Z}^T\nabla f(q_p) \| = 0 \tag{12}$$

Equation (12) shows that at the optimal condition, the vector of the objective functions gradient and the active constraints null space are orthogonal to each other. For full mathematical explanation and proofs on constrained optimization with active set, see Griva et al. (2009).

Applied for Jet Pump Network

The reduced Newton method with active constraints to a jet pump network of oil wells is now applied. Generic equations above are written specifically for a jet pump network. The objective function is multiplied by negative one to turn it into a

minimization. This allows methods from Griva et al. (2009) to be applied since all problems in the text are minimized.

$$\begin{aligned} \text{minimize } & f(q_p) = \sum_{i=1}^{n} -c_{1i} + c_{2i} \exp\left(-q_{pi} c_{3i}\right) \\ \text{subject to } & \sum_{i=1}^{n} q_{p\,i} \leq Q_{\mathrm{p}}^{\mathrm{pump}} \\ & q_{p\,i} \geq 0 \end{aligned}$$

Gradient of the objective function is a first derivative of each well with respect to its own power fluid.

$$\nabla f(q_p) = \begin{pmatrix} -c_{21} c_{31} \exp\left(-q_{p1} c_{31}\right) \\ \ldots \\ -c_{2n} c_{3n} \exp\left(-q_{pn} c_{3n}\right) \end{pmatrix}$$

Hessian of the objective function is a diagonal matrix of a second derivative of each well with respect to its own power fluid.

$$\nabla^2 f(q_p) = \begin{pmatrix} c_{21} c_{31}^2 \exp\left(-q_{p1} c_{31}\right) & 0 & 0 \\ 0 & \ldots & 0 \\ 0 & 0 & c_{2n} c_{3n}^2 \exp\left(-q_{pn} c_{3n}\right) \end{pmatrix}$$

Top n rows of constraint matrix A and vector b represent individual wells. Bottom $n+1$ row represents total power fluid limitation. Bottom row is multiplied by negative one so all rows adhere to $Ax \geq b$. The letter k is an iteration counter.

$$A = \begin{pmatrix} 1 & 0 & 0 \\ 0 & \ldots & 0 \\ 0 & 0 & 1 \\ -1 & -1 & -1 \end{pmatrix} \quad q_p^k = \begin{pmatrix} q_{p1} \\ \ldots \\ q_{pn} \end{pmatrix} \quad b = \begin{pmatrix} 0 \\ \ldots \\ 0 \\ -Q_p^{pump} \end{pmatrix}$$

To start the optimization scheme, a feasible point must be selected. To begin, power fluid is evenly distributed among wells following $q_{pn} = Q_p^{pump}/n$. As a result, only the bottom row is active in A and b.

$$\hat{A} = \begin{pmatrix} -1 & \ldots & -1 \end{pmatrix} \quad q_p^0 = \begin{pmatrix} \frac{Q_p^{pump}}{n} \\ \cdots \\ \frac{Q_p^{pump}}{n} \end{pmatrix} \quad \hat{b} = \begin{pmatrix} -Q_p^{pump} \end{pmatrix}$$

In the following application, QR factorization is used to find the null space of active constraints. Results from the QR method can also be used to find Lagrange multiples without much additional computation required. Again, Griva et al. (2009) should be used for details.

Discrete Jet Pump Selection

The method described above optimizes a continuous variable, the power fluid. In reality, the system is discrete, as specific jet pumps are installed which control flow of power fluid. Recommended power fluid from the continuous optimization is bounded by a low power fluid jet pump and a high power fluid jet pump. The final step is to select which of the two jet pumps will be installed for each well.

The solution is defined by initially assuming all low power fluid jet pumps will be installed. This guarantees that total power fluid volume is lower than pump capacity. The problem then becomes selecting which jet pumps to convert from low power to high power fluid without exceeding the surface pump's residual capacity, Q_p^{res}. This discrete selection problem is commonly referred to as the 0-1 knapsack problem.

$$\begin{aligned} \text{maximize} \sum_{i=1}^{n} x_i \Delta q_{o\,i} \\ \text{subject to} \sum_{i=1}^{n} x_i \Delta q_{p\,i} \leq Q_{\mathrm{p}}^{\mathrm{res}} \\ x_i \in \{0, 1\} \end{aligned}$$

Where x_i is selecting the high power fluid jet pump, categorized as 0 for the low pump and 1 for the high. Terms Δq_o and Δq_p are differences in oil and power fluid between selecting the high and low power fluid jet pump. Mathematically described as $\Delta q_o = q_{o,high} - q_{o,low}$ and $\Delta q_p = q_{p,high} - q_{p,low}$.

A greedy algorithm is selected to solve the 0-1 knapsack problem because of its lower computational cost compared to other algorithms (Martello and Toth 1990). The greedy algorithm does not guarantee the maximized solution, but as this part of the algorithm is tertiary, the trade off in performance is accepted.

Example

The optimization methodology was applied at a drill site in the Milne Point field of Alaska. The artificial lift method at the drill site is a mixture of electric submersible pumps and jet pumps. The drill site has its own production separator and power fluid pump which act as a jet pump network for eight wells. A few months prior to the analysis, a series of grass roots production wells were drilled at the site. Based on calculations before the optimization scheme was developed, it was concluded that the network could only support eight wells on jet pump. As a result, one of the grass roots wells was completed as an electric submersible pump (esp) and the other wells as jet pumps.

During surveillance of the electric submersible pump, it was noted that its ability to draw down the well was less than it's adjacent jet pumps. The operator wanted to swap the well from electric submersible to jet pump, but did not know how other jet pump wells would be impacted. Inflow performance showed that the well could produce 1250 bopd using a jet pump. To fully understand performance, the optimization scheme was first deployed on the existing well configuration. These results are compared to adding the esp well as a jet pump.

Number	Type	Size	Oil	FWC	FGOR	c1	c2	c3
15	JP	11B	274.7	49.9	1172	353.7	230.8	9.62e-4
17	JP	12B	378.3	67.6	931	578.9	430.4	5.64e-4
26	JP	13C	443.8	28.5	409	835.5	506.1	5.69e-4
27	JP	12B	734.8	18.6	341	834.5	674.0	8.63e-4
29	JP	14C	1188.4	3.5	190	1127	980.2	5.98e-4
31	JP	14C	1037.1	49.8	862	944.5	807.5	6.89e-4
33	JP	14C	1205.5	31.1	978	1237	1226	7.35e-4
36	JP	14C	1162.9	33.3	592	1262	858.6	4.63e-4
22	ESP	NA	852.2	26.2	295	NA	NA	NA

Table 3: Drillsite Production Wells

The surface network pump has a max capacity of 32000 bwpd with a discharge pressure of 3400 psig, which is at the max allowable operating pressure of the piping. It was decided to keep the capacity and discharge pressure of the network pump at a fixed setting in the optimization scheme to simplify the analysis. The scheme could be run at different power fluid pressures and rates, but that would complicate the problem.

Results

The continuous optimization scheme is first run on the base jet pump wells. Figure 8 shows the base jet pump wells run, where iteration 1 is starting with an even distribution of power fluid to each well. The left is the total estimated oil rate

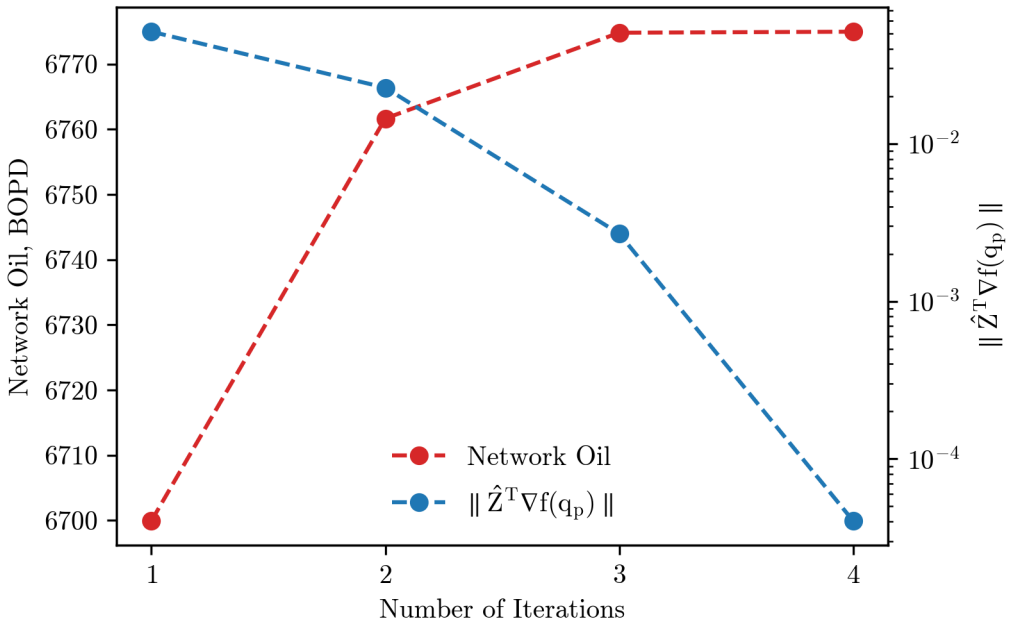

Figure 8: Convergence of Oil Produced and Optimality Condition

coming from the network. On the right is the optimality condition, shown in equation (12). The program terminates when the optimality condition is below a tolerance of 1E-3. The continuous optimization scheme is fast, taking advantage of the quadratic behavior of the Newton method to converge in four iterations.

The esp well is modeled as a jet pump using bottom hole gauge and well test data. Coefficients for well 22 are estimated to be c1: 1237, c2: 1226 and c3: 7.3e-4. These coefficients and modeling supported prior to ideas that the well would produce approximately 1250 bopd as an esp. The well is then added to the existing network and the continuous scheme is rerun.

Name	Eight Wells BOPD	Well 22 BOPD	Type	Total BOPD
Base Run	6774	852	ESP	7627
Conversion	6619	1176	JP	7796
Difference	-155	+324	JP	+169

Table 4: Network Run Results

Shown in table 4 are results from two different runs. As seen, oil rate of the eight base jet pump wells fell by 155 bopd, while the esp conversion itself resulted in an addition of 324 bopd. Adding an impact on the eight base wells and benefit for jet pump conversion results in a net positive of 169 bopd. Results are then passed into the discrete algorithm to select the different jet pumps for use. The discrete jet pump optimization recommended jet pumps to be run are shown in table 5.

Number	Size	Oil BOPD	Power Fluid BWPD
15	**9E**	253	1445
17	12B	490	2887
26	**11D**	426	2354
27	**13C**	794	3886
29	14C	1217	4814
31	**13C**	813	3768
33	**13C**	978	3731
36	14C	1179	4850
22	**13C**	1277	3754

Table 5: Discrete Jet Pump Selection

Values in bold highlight which jet pumps geometries are changed out. Wells 15 and 17 had reductions in nozzle size with increases in throat ratios. An increase in throat ratio allows more flow to pass, but doesn't benefit from as much head. Wells 31 and 33 had reductions in nozzle sizes while maintaining the same throat ratio. Interestingly, the algorithm recommended up sizing well 27's jet pump from a 12B to a 13C. This was attributed to the 12B significantly choking well 27.

Conclusion

A new method of optimizing power fluid in jet pump oil wells is established and explained. The algorithm uses a reduced Newton direction with active set constraints for continuous optimization. Constraints are set up to handle a total power fluid limit as well as non-negative limit for each well. If desired, constraints could easily be added for minimum and maximum allowable power fluid per well. Output from the continuous optimization is passed to a discrete algorithm for selecting each jet pump. The discrete algorithm makes use of the 0-1 knapsack to select between two different jet pumps per well.

The optimization algorithms are built on top of numerical methods for modeling fluid flow through jet pumps. Numerical methods capture the reservoir fluids density changes related to pressure and flow limits encountered from sonic velocity constraints. This is a significant improvement from current industry methodologies that use analytical methods by Petrie et al. (1983b). Since the calculations required to apply numerical methods are large, a computer program was developed to handle optimization and jet pump modeling.

A field example of an eight jet pump well network was presented. The optimization scheme helped the field operator answer the question of whether an esp well should be converted to jet pump. The operator was unsure of how the well would perform on jet pump and its impact to the other existing producers. Analysis showed that converting the well resulted in a net improvement on oil production, and the project was sanctioned.

Optimization and modeling proposed in this paper marks an important transition in jet pump applications. As more oil fields target cold, shallow, viscous reservoirs, it is expected that the use of jet pumps and their associated networks will increase. Authors of this paper hope it helps operators allocate power fluid volumes for jet pump oil wells. It is also our hope that this paper inspires others to improve the methodology discussed above.

Nomenclature

Fluid and Mechanical

$\dot{m}$	Mass Flow, lb_m/s
Ma	Mach Number
Re	Reynolds Number
$\forbar{V}$	Specific Volume, ft^3/lb_m
a	Speed of sound, ft/s
ρ	Density, lb_m/ft^3
A	Area, ft^2
E	Energy Density, ft^2/s^2
K	Friction Factor, unitless
P	Pressure, psia
V	Velocity, ft/s

Fluid Subscripts

di	Diffuser
ni	Nozzle Inlet
nz	Nozzle
su	Suction
te	Throat Entry
th	Throat
tm	Throat Mixture

Numerical Subscripts

i	Specific Well Reference
k	Iteration Counter
n	Total Wells in Network

Optimization

$\nabla f(q_p)$	Gradient of Obj. Function
$\nabla^2 f(q_p)$	Hessian of Obj. Function
A	Constraint Matrix
b	Constraint Vector
$f(q_p)$	Objective Function
p	Search Direction
Q_p^{pump}	Surface Pump Power Fluid
q_o	Vector of Oil Rates
q_p	Vector of Power Fluids
x	Discrete Jet Pump Selection
Z	Null Space of Constraints

Appendix

A Throat Entrance Equation

The following appendix provides a derivation for the jet pump throat entry, equation (2) and (6), from the main document. The jet pump energy, equation (1), is integrated across from suction to the throat entry.

$$\int_{su}^{te} \frac{dP}{\rho} + \int_{su}^{te} VdV + \int_{su}^{te} dF = 0 \tag{A1}$$

The following simplifying assumptions are applied.

1. Velocity of the fluid at suction conditions is negligible
2. Friction is represented by Cunningham friction coefficients

The following complexities are maintained.

1. Density and differential pressure relationship of the multiphase mixture

$$\int_{su}^{te} \frac{dP}{\rho} + \frac{V_{te}^2}{2} - \frac{\cancel{V_{su}^2}}{\cancel{2}} + K_{te}\frac{V_{te}^2}{2} = 0 \tag{A2}$$

Rewriting in the simplest analytical form.

$$\int_{su}^{te} \frac{dP}{\rho} + \frac{V_{te}^2}{2} * (1 + K_{te}) = 0 \tag{A3}$$

The trapezoid rule is applied as a numerical integration approximation to describe the density of the oil mixture with changes in pressure. ΔP is a user input that controls the granularity of the numerical approximation.

$$\frac{\Delta P}{2} \sum_{k=su}^{te} (\frac{1}{\rho_k} + \frac{1}{\rho_{k+1}}) + \frac{V_{te}^2}{2} * (1 + K_{te}) = 0 \tag{A4}$$

B Nozzle Equation

The following appendix provides a derivation for jet pump nozzle, equation (3) from the main document. The jet pump energy, equation (1), is integrated across from the nozzle inlet to the nozzle tip.

$$\int_{ni}^{nz} \frac{dP}{\rho} + \int_{ni}^{nz} VdV + \int_{ni}^{nz} dF = 0 \tag{B1}$$

The following simplifying assumptions are applied.

1. Density of the power fluid is incompressible water
2. Velocity of the nozzle inlet is negligible
3. Friction is represented by Cunningham friction coefficients

$$\frac{P_{nz}}{\rho_{nz}} - \frac{P_{ni}}{\rho_{nz}} + \frac{V_{nz}^2}{2} - \cancel{\frac{V_{ni}^2}{2}} + K_{nz}\frac{V_{nz}^2}{2} = 0 \tag{B2}$$

Multiplying through by the density and writing the equation in terms of P_{nz}.

$$P_{nz} = P_{ni} - \frac{\rho_{nz} V_{nz}^2}{2} * (1 + K_{nz}) \tag{B3}$$

The pressure at the nozzle is assumed to be the same as the pressure at the throat entrance, giving the final version of the nozzle equation.

$$P_{te} = P_{ni} - \frac{\rho_{nz} V_{nz}^2}{2} * (1 + K_{nz}) \tag{B4}$$

C Throat Equation

The following appendix provides a derivation for the jet pump throat mixing, equation (4) from the main document. The fixed control volume linear momentum equation is used to represent the nozzle. Section 3.4 *Linear Momentum Equation* from White (2011) should be consulted for more information.

$$\sum \mathbf{F} = \frac{d}{dt}\int_{CV} V\rho \, d\cancel{V} \; + \int_{CS} V\rho \, (V \cdot \hat{n}) \, dA \tag{C1}$$

For a steady state and one dimensional flow, the equation simplifies to.

$$\sum \mathbf{F} = \sum (\dot{m}V)_{out} - \sum (\dot{m}V)_{in} \tag{C2}$$

Writing in terms of the jet pump throat. Where τA_w is the shear force imparted on the throat wall by the fluid.

$$P_{te}A_{th} - P_{tm}A_{th} - \tau A_w = \dot{m}_{tm}V_{tm} - \dot{m}_{nz}V_{nz} - \dot{m}_{te}V_{te} \tag{C3}$$

According to Cunningham (1995) the shear stress along the wall is rewritten as:

$$\frac{\tau A_w}{A_{th}} = \frac{\rho_{tm} V_{tm}^2 K_{th}}{2} \tag{C4}$$

Placing the shear stress on the right and substituting in (C4) yields the throat force balance.

$$P_{te} - P_{tm} = \frac{\rho_{tm} V_{tm}^2 K_{th}}{2} + \frac{\dot{m}_{tm}V_{tm}}{A_{th}} - \frac{\dot{m}_{nz}V_{nz}}{A_{th}} - \frac{\dot{m}_{te}V_{te}}{A_{th}} \tag{C5}$$

D Diffuser Equation

The following appendix provides a derivation for the jet pump diffuser, equation (5), from the main document. The jet pump energy, equation (1), is integrated across from the throat mixture to the diffuser.

$$\int_{tm}^{di} \frac{dP}{\rho} + \int_{tm}^{di} V dV + \int_{tm}^{di} dF = 0 \tag{D1}$$

The following simplifying assumptions are applied.

1. Friction is represented by Cunningham friction coefficients

The following complexities are maintained.

1. Velocity of the throat mixture
2. Density and differential pressure relationship of the multiphase mixture

$$\int_{tm}^{di} \frac{dP}{\rho} + \frac{V_{di}^2}{2} - \frac{V_{tm}^2}{2} - K_{di}\frac{V_{tm}^2}{2} = 0 \tag{D2}$$

Rewriting in the simplest analytical form.

$$\int_{tm}^{di} \frac{dP}{\rho} + \frac{V_{di}^2}{2} - \frac{V_{tm}^2}{2} * (1 + K_{di}) = 0 \tag{D3}$$

The trapezoid rule is applied as a numerical integration approximation to describe the density of the oil mixture with changes in pressure. ΔP is a user input that controls the granularity of the numerical approximation.

$$\frac{\Delta P}{2} \sum_{k=tm}^{di} (\frac{1}{\rho_k} + \frac{1}{\rho_{k+1}}) + \frac{V_{di}^2}{2} - \frac{V_{tm}^2}{2} * (1 + K_{di}) = 0 \tag{D4}$$

E Gradient of the Throat Entry Energy vs Pressure

The following appendix provides a derivation for equation (7) from the main document. Three fundamental equations are used when assessing change in energy of the throat entrance versus the change in pressure. The equations are the differential friction-less throat entry energy (E1), differential conservation of mass (E2), and sonic velocity of a fluid (E3).

$$dE_{te} = \frac{dP}{\rho} + VdV \tag{E1}$$

$$\frac{d\rho}{\rho} + \frac{dV}{V} + \frac{dA}{A} = 0 \tag{E2}$$

$$a^2 = \frac{dP}{d\rho} \tag{E3}$$

The fluid sonic velocity (E3) is written as $dP = a^2 d\rho$ and substituted into $\mathrm{dE_{te}}$ (E1) for dP.

$$dE_{te} = \frac{a^2 d\rho}{\rho} + VdV \tag{E4}$$

The entire equation is divided through by a^2 and the last term is multiplied by V/V.

$$\frac{dE_{te}}{a^2} = \frac{d\rho}{\rho} + \frac{V^2}{a^2}\frac{dV}{V} \tag{E5}$$

In this specific application the analysis is exactly at the throat entry and investigating how its energy changes with pressure. As such, the differential area term is 0 in equation (E2). The equation is rewritten by moving $d\rho/\rho$ to the right side.

$$\frac{dV}{V} = -\frac{d\rho}{\rho} \tag{E6}$$

In equation (E5) it is recognized that $\mathrm{Ma}^2 = V^2/a^2$. Additionally equation (E6) is substituted into (E5).

$$\frac{dE_{te}}{a^2} = \frac{d\rho}{\rho} - \mathrm{Ma}^2\frac{d\rho}{\rho} \tag{E7}$$

The parameter $d\rho/\rho$ is factored out of equation (E7) and then divided by $d\rho$.

$$\frac{dE_{te}}{a^2 d\rho} = \frac{1}{\rho}(1 - \mathrm{Ma}^2) \tag{E8}$$

Equation (E3), the sonic velocity, is substituted into equation (E8) in the form $a^2 d\rho = dP$.

$$\frac{dE_{te}}{dP} = \frac{1}{\rho}(1 - \mathrm{Ma}^2) \tag{E9}$$

Equation (E9) provides the final form and describes the behavior of $\mathrm{dE_{te}}$ versus changes in pressure. It should noted that the original form of $\mathrm{dE_{te}}$ was idealized, as friction was not included. Nonetheless, equation (E9) demonstrates that the slope of E_{te} vs pressure will change once the sonic boundary is activated. This matches performance found in the numerical analysis of E_{te} and traditional analysis of flow properties at sonic conditions (White 2011).

References

Armijo, Larry. 1966. Minimization of Functions having Lipschitz Continuous First Partial Derivatives. *Pacific Journal of Mathematics* 16, no. 01 (November). https://doi.org/10.2140/pjm.1966.16.1.

Cunningham, R. G. 1974. Gas Compression with the Liquid Jet Pump. *ASME J. Fluids Eng.* 96, no. 3 (September): 203–215. https://doi.org/10.1115/1.3447143.

Cunningham, R. G. 1995. Liquid Jet Pumps for Two-Phase Flows. *ASME J. Fluids Eng.* 117, no. 2 (June): 309–316. https://doi.org/10.1115/1.2817147.

Gilat, Amos, and Vish Subramaniam. 2013. Numerical Methods for Engineers and Scientists 3rd Ed. Chap. 9. Wiley.

Griva, Igor, Stephen Nash, and Ariela Sofer. 2009. Linear and Nonlinear Optimization 2nd Ed. Chap. 15.2 - 15.4, 549–570. SIAM Press.

Himr, Daniel, Vladimir Haban, and Frantisek Pochyly. 2009. Sound Speed in the Mixture Water - Air. In *Engineering mechanics conference.* Svratka, Czech Republic, May.

Holland, FA, and R Bragg. 1995. Fluid Flow for Chemical Engineers. Chap. 6, 189–190. 338 Euston Road, London NW1 3BH: Edward Arnold.

Martello, Silvano, and Paolo Toth. 1990. Knapsack Problems. Chap. 2.4. John Wiley and Sons.

Merrill, Robert, Vivek Shankar, and Thomas Chapman. 2020. Three-Phase Numerical Solution for Jet Pumps Applied to a Large Oilfield. In *Abu dhabi international petroleum exhibition and conference.* November. https://doi.org/10.2118/202928-MS.

Payne, G.A., C.M. Palmer, J.P. Brill, and H.D. Beggs. 1979. Evaluation of Inclined-Pipe, Two-Phase Liquid Holdup and Pressure-Loss Correlation using Experimental Data. *Journal of Petroleum Technology* 31, no. 09 (September). https://doi.org/10.2118/6874-PA.

Petrie, Hal, Phil Wilson, and Eddie Smart. 1983a. Jet Pumping Oil Wells, Part 1 Design Theory, Hardware Options and Application Considerations. *World Oil* 197, no. 6 (November).

Petrie, Hal, Phil Wilson, and Eddie Smart. 1983b. Jet Pumping Oil Wells, Part 2 Hand-held Computer Programs for Installation Design. *World Oil* 198, no. 7 (December).

Sanger, Nelson L. 1968. *Noncavitating Performance of Two Low-Area-Ratio Water Jet Pumps having Throat Lengths of 7.25 Diameters.* Technical report. National Aeronautics and Space Administration, March.

Verma, Sumil Kumar, Shiv Prakash Ojha, Mihir Jha, et al. 2014. The Importance of Critical Flow Considerations in Understanding Jet Pump Performance: The Mangala Field. In *Iptc international petroleum technology conference.* December. https://doi.org/10.2523/IPTC-18167-MS.

Vogel, J.V. 1968. Inflow Performance Relationships for Solution-Gas Drive Wells. *Journal of Petroleum Technology* 20, no. 01 (January): 83–92. https://doi.org/10.2118/1476-PA.

White, Frank. 2011. Fluid Mechanics 7th Ed. Chap. 9, 622–623. 1221 Avenue of the Americas, New York, NY 10020: McGraw-Hill.